# Visual Support to Filtering Cases for Process Discovery

Luiz Schirmer, Leonardo Quatrin Campagnolo, Sonia Fiol González, Ariane M. B. Rodrigues,
Guilherme G. Schardong, Rafael França, Mauricio Lana,
Simone D. J. Barbosa, Marcus Poggi and Hélio Lopes
*Pontifícia Universidade Católica do Rio de Janeiro,*
*Departamento de Informática, Rio de Janeiro, RJ, Brazil*

Keywords: Visual Filtering, Process Mining, Event Log, Multidimensional Projection.

Abstract: Working with average-sized event logs is still a major task in process mining, where the main goal is to gain process-related insights based on event logs created by a wide variety of systems. An event log contains a sequence of events for every case that was handled by the system. Several discovery algorithms have been proposed and work well in specific cases but fail to be generic strategies. Moreover, there is no evidence that the existing strategies can handle events with a large number of variants. For this reason, a generic approach is needed to allow experts to explore event log data and decompose information into a series of smaller problems, to identify outliers and relations between the analyzed cases. In this paper we present a visual filtering approach for event logs that makes process analysis tasks more feasible and tractable. To evaluate our approach, we have developed a visual filtering tool and used it with the event log from BPI Challenge 2017.



## 1 INTRODUCTION

The business world is complex: various actors are involved in designing, delivering, and offering services (Mendling et al., 2017), and the knowledge of how these processes behave is essential in the field of Business Process Management (BPM). BPM is related with the management activities around daily business processes. During the last decade, the need for companies to learn more about how their processes work in the real world has increased the use of Process Mining techniques (Tiwari et al., 2008). Grounded in the data mining field, such techniques aim to retrieve relevant information from the analyzed workflow. Among the topics used in data-driven process analysis, we highlight Process Discovery, Conformance Checking, and Process Improvement (Van der Aalst, 2016).

Information retrieval related to BPM aims to answer several questions to support making decisions and managing process execution by offering several features, such as analysis, prediction, monitoring, control, and optimization.

Following a bottom-up approach, process mining deals with information gathered as the processes are executed, recording events of each case as they occur, and then building a structured process description from those recorded events (Van der Aalst and Weijters, 2004). In sum, process mining is a research field that acts on the intersection of methods like machine learning, data mining, and BPM (Van der Aalst, 2016).

In the field of Process Discovery, we aim to get an actual event log and create another controlled structure, such as a workflow, which represents most of the cases captured by that log. When dealing with simple examples, the reconstruction of a workflow can be quite easy. However, for large workflow models this can be much more difficult (Van der Aalst et al., 2004). A recent approach to deal with large datasets consists of simplifying the large event log into smaller sublogs, applying the discovery algorithm to these sublogs, and then merging the results to generate a solution to the whole system. By mining smaller logs and later merging the (sub)solutions, this approach significantly speeds the discovery algorithm (Verbeek et al., 2017). With this in mind, we want to expand the range of approaches that simplify a model to make it easier to understand.

In recent years, various techniques were proposed to visualize and generate clusters of BPM data. Most of these techniques focus on optimizing soluti-



Schirmer, L., Quatrin Campagnolo, L., Fiol González, S., M. B. Rodrigues, A., G. Schardong, G., França, R., Lana, M., D. J. Barbosa, S., Poggi, M. and Lopes, H.
Visual Support to Filtering Cases for Process Discovery.
DOI: 10.5220/0006708200380049
In *Proceedings of the 20th International Conference on Enterprise Information Systems (ICEIS 2018)*, pages 38-49
ISBN: 978-989-758-298-1

ons based on a similarity measure between traces of data, i.e., the event log is split into homogeneous subsets and for each subset a process model is created (De Koninck and De Weerdt, 2016). In this paper, we propose a new visual filtering approach to event logs, based on multidimensional projection techniques. With this approach, we create a lower dimensional representation of the cases, preserving their dissimilarity to one another, and visually select the ones that stand out or spark interest. Then, we generate a new, filtered event log using only the selected cases. Such event log can then be further analyzed using standard process mining approaches.

The main contribution of our work is a visual approach for filtering processes based on their low dimensionality representation. Our second contribution is the proposal of a dissimilarity function that uses not only the attributes of the process cases, but also the dissimilarity of their paths. Our third and final contribution involves the use of entropy to analyze the variability of the processes' attributes. With those contributions, we expect that our work can be used as a support tool for process discovery.

The remainder of this paper is organized as follows: Section 2 presents related work. Next, in Section 3 we introduce the main components of our approach and explain the visualization techniques employed. Section 4 introduces the filtering tool proposed, as well as the interaction mechanisms provided. Section 5 presents an application of the proposed approach using real process data in order to demonstrate its advantages. Finally, Section 6 presents some concluding remarks and directions for future works.

## 2 RELATED WORK

In the past, activities related to BPM were conducted by process analysts with almost no automatic support for process modeling (Mendling et al., 2017). This has been changing with the creation of new techniques and algorithms developed to automate or provide intelligent support for process mining and process analysis. The visualization of cases from an event log, however, still presents challenges.

To overcome problems related to data analysis and visualization, Van Dongen *et al.* (2005) have developed the ProM framework, an extensible environment for process mining. The system is flexible with respect to input and output parameters, and easy to reuse code during the implementation of new process mining features. It combines different techniques for data mining and process flow analysis. However, with Prom it is not possible to look at the log and group cases by attributes similarities.

Verbeek *et al.* (2017) proposed a generic approach to group similar sequences of activities, splitting a unique event log file into a number of event logs with fewer variants each. This was implemented as a plug-in in ProM6 and allows for easier decomposed discovery, using six different discovery algorithms. For the decomposed discovery, the framework allows the end user to select the classifier, which maps the event log at hand onto an activity log; the miner (or discovery algorithm); and a configuration.

Low *et al.* (2017) have developed visualization techniques to provide targeted analysis of resource reallocation and activity rescheduling. They have analyzed differences between event logs and the changes are conceptualized and realized with a number of visualizations. Using such visualizations, analysts can identify resource and time-related changes, which result in a cost reduction of the process, and investigate them further. They use social network graphs to illustrate the reallocation of resources and a timeline visualization approach to depict time-related information and identify temporal patterns. Moreover, the system provides a clear view of two event logs side-by-side, so that differences and similarities can be visually identified. However, the proposed system does have some issues. With a large number of variants and cases, it is difficult to identify issues in the data with a visual analysis. In some cases, the use of the graph and the timeline visualization can confuse the users (Low et al., 2017).

To solve some of the aforementioned issues, we developed a visual interactive filtering tool which allows the generation of smaller event logs by selecting a subset of cases. Contrasting with the approach of Verbeek *et al.* (2017), presented in Figure 1, we create a visual application to filter cases and generate sublogs. Our strategy can be considered more flexible and tractable than theirs, as in our approach domain experts and analysts can freely explore and analyze the data, and then create sublogs according to their insights.

## 3 VISUAL FILTERING APPROACH

Our visual filtering approach is based on evaluating the difference between cases using a set of attributes. There is a multitude of metrics available to accomplish this. Paixão *et al.* (2009) propose the use of weighted additive distances to denoise a vector field. We adapt this metric to our problem, where each attribute $f$ of a case receives a weight $\alpha_f \in [0,1]$. We

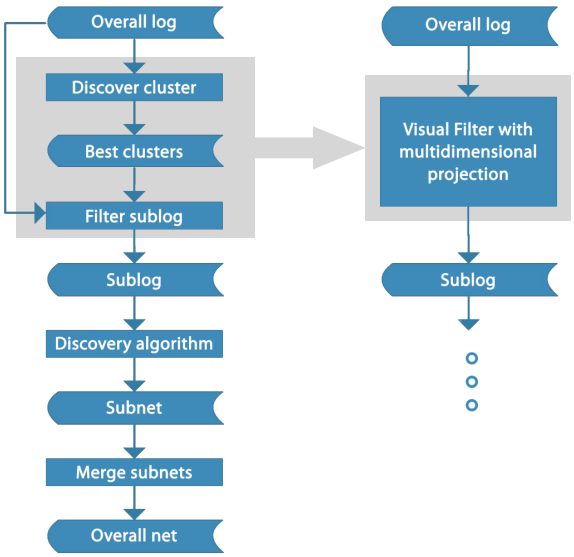


Figure 1: Conceptual view of a decomposed discovery algorithm given by (Verbeek et al., 2017) and our proposed approach.

calculate the similarity between each attribute of two cases $i, j | i \neq j$ and weigh that attribute's importance using $\alpha_f$. The product of each attribute similarity for cases $i, j$ results in a measure of similarity between the cases. Subtracting this value from 1 gives a measure of the dissimilarity between $i$ and $j$, as defined in Equation 1,

$$d_{i,j} = 1 - \prod_{f=0}^{|F|} \left[ e^{-\alpha_f (f_i - f_j)} \right] \quad (1)$$

where $F$ is the attribute set, $(i, j) | i \neq j$ are the $i$-th and $j$-th case, $|F|$ is the cardinality of the attribute set, $\alpha_f$ is a weight factor associated to attribute $f \in F$ and $f_i - f_j$ is the difference between attribute $f$ of cases $i$ and $j$. When dealing with categorical variables, the $f_i - f_j$ term is replaced by a boolean comparison between the categories, which means that we argue whether $f_i == f_j$.

We have also implemented two measures to calculate the distance between the path of two cases: the Levenshtein distance and the Jaccard index. The Levenshtein distance, or edit distance, measures the minimum number of operations needed to transform a string into another (Levenshtein, 1966). Here, the insertion, removal or change of characters are considered as valid operations. For example, the edit distance between case $I$ with an activity sequence of $ABCD$ and case $J$ with an activity sequence of $ABDE$ is 2, since activity $C$ of $I$ would be converted to $D$ and activity $D$ of $I$ would be converted to $E$. Equation 2 presents the mathematical definition of the Levenshtein distance.

$$L_{I,J}(a,b) = \begin{cases} max(a,b) & min(a,b) = 0 \\ \begin{cases} L(a-1,b)+1 \\ L(a,b-1)+1 \\ L(a-1,b-1)+1_{(I_a \neq J_b)} \end{cases} & otherwise \end{cases} \quad (2)$$

where $I$ and $J$ are two different cases, $a$ and $b$ are activities belonging to case $I$ and $J$ respectively and $1_{(I_a \neq J_b)}$ is the indicator function, resulting in 0 if $I_a = J_b$ and 1 otherwise.

The Jaccard index measures the fraction of common samples between two finite sets of samples and is defined by the number of common samples divided by the total number of samples in both sets (Jaccard, 1901). We applied this metric by considering that each case is composed of a set of activities. Thus, to measure the dissimilarity between cases $I$ and $J$, we subtracted their Jaccard index from 1. Equation 3 presents the definition of the Jaccard dissimilarity.

$$J(i,j) = 1 - \frac{|I \cap J|}{|I \cup J|} \quad (3)$$

In order to visually assess the similarity between the cases, we employ two multidimensional projection techniques: Multidimensional Scaling (MDS) (Kruskal and Wish, 1978) and t-Stochastic Neighbor Embedding (t-SNE) (Maaten and Hinton, 2008). MDS is a set of algorithms aimed at providing a lower dimensionality representation of a distance matrix. The main goal is to create a simpler representation of the cases, but maintaining their relative distances as close to the original values as possible.

The classical MDS algorithm uses an eigenvalue decomposition of the distance matrix to calculate a coordinate matrix in a lower dimensionality space. This approach requires a full representation of the distance matrix, which is costly in terms of memory usage. In addition, the eigenvalue decomposition is performed by using the power iteration, or power method (Mises and Pollaczek-Geiringer, 1929), which in turn is a computationally costly algorithm. Wickelmaier (2003) provides a good intuition on this particular algorithm, as well as worked examples.

The primary outcome of an MDS projection is a spatial configuration, in which the objects are represented as points and arranged in such a way that their euclidean distances correspond to the dissimilarities of the objects in the original space, i.e., similar objects are represented by points that are close to each other, whereas dissimilar objects by points that are further apart. A prominent application of MDS is the visualization of high-dimensional correlational data, such as data from process cases.

The weights assigned to each attribute in Equation 1 have direct influence on the dissimilarity matrix and its eigenvalue decomposition. This leads to different spatial configurations for different sets of weights. A careful study of the attributes variability and subsequent weight assignments may lead to a configuration that naturally highlights the different groups in the data, such as the one presented in Figures 2 and 7.

The second multidimensional projection technique employed is called t-Distributed Stochastic Neighbor Embedding (t-SNE) (Maaten and Hinton, 2008). The goal of this technique is to embed high dimensional data into a low dimensional space, typically of 2 or 3 dimensions. Since its inception, it became widely popular to visualize results of machine learning techniques (Wattenberg et al., 2016). t-SNE builds upon the original Stochastic Neighbor Embedding (SNE) algorithm, proposed by Hinton and Roweis (2003). Both t-SNE and SNE work in two stages: First, they convert the pairwise dissimilarities between the data points in the high-dimensional space into conditional probabilities, such that points with small dissimilarities will have a high probability of being neighbors and points with large dissimilarities will have a lower probability of being neighbors. The second stage involves the same construction, only for the low dimensional space. The algorithm then proceeded by minimizing the sum of Kullback-Leibler divergences between these two probability distributions. However, SNE suffers from two problems that motivated the creation of t-SNE: The Kullback-Leibler divergence function is difficult to minimize; and a so-called "Crowding problem". Both problems are heavily detailed by van der Maaten and Hinton (2008). t-SNE partially solves both problems by proposing a joint probability distribution, called symmetric SNE, which solves the Kullback-Leibler minimization issues; and by proposing the use of a Student t-distribution to map dissimilarities onto probabilities in the low dimensional space, alleviating the crowding problem (Maaten and Hinton, 2008).

In practical terms, t-SNE is capable of revealing both local and global aspects of the data. However, as stated by Wattenberg et al. (2016), t-SNE is heavily dependent on the input parameters, and may show group structures where there are none, besides deforming existing groups, misrepresenting their true size and inter-group distance.

Figures 2 and 3 show the results of applying the MDS and t-SNE algorithms, respectively, over the same 3,000 cases sampled uniformly at random.

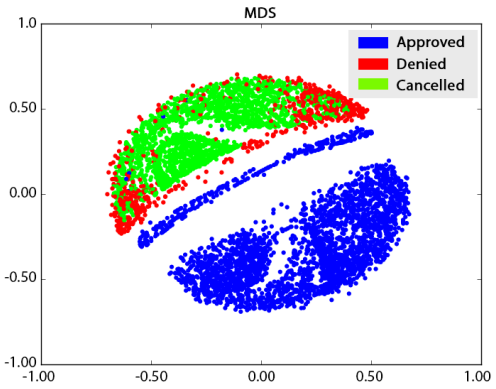


Figure 2: Our proposed case filtering visualization using MDS projection using 3,000 cases.

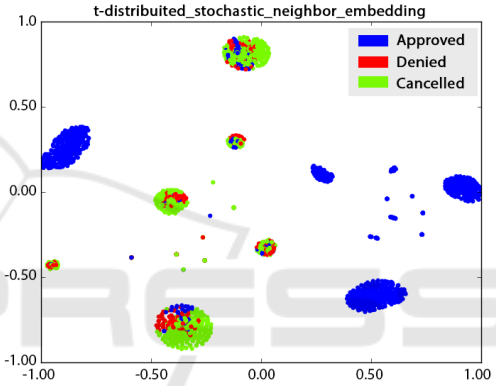


Figure 3: Our proposed case filtering visualization for t-SNE projection with 3,000 cases and a perplexity of 50.

## 4 VISUAL FILTERING TOOL

Our filtering tool comprises a set of 2D charts (MDS and t-SNE), onto which we project the cases, and a set of user interface elements to adjust visibility and weight parameters. Figure 4 shows a prototype of our tool with some cases plotted. Using the sliders, we can define the $\alpha_f$ weight for each feature included in the measure of dissimilarity presented in Equation 1.

Besides the features, it is important to know all activities of each case. A case can be considered undefined if, when analyzing the event log, its end is not identified. In our approach, we consider all case types with a defined endpoint, *i.e.*, either successful or unsuccessful. We can group cases into different sets of points, using a specific marker for each group. In Figure 4, we project cases which ended in success (Approved), denial (Denied) or cancellation (Cancelled). It is essential to be able to filter and group the data, so we can later use them to retrieve information

about the identified groups.

Given the log projected into a 2D chart, we may select multiple cases, as exemplified in Figure 5. We can also select multiple cases based on projections generated with different weights for each feature. Then, we can export a CSV file with the filtered cases to be used in a process mining software, such as ProM (Verbeek et al., 2010) and Fluxicon Disco (Mining, 2014). These softwares help analyze the activity flow of the cases.

Our visual filtering tool was implemented in Python using Sklearn and Matplotlib Packages (Pedregosa et al., 2011; Hunter, 2007).

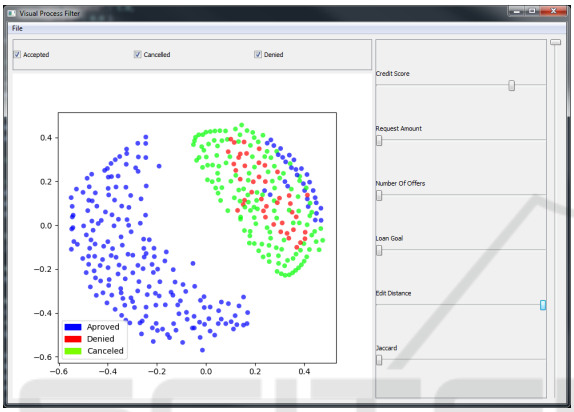


Figure 4: Our visual filtering prototype with 400 cases.

## 5 APPLYING VISUAL FILTERING

Process mining results reveal what goes on inside processes and can be used to diagnose problems and suggest solutions (Van Der Aalst, 2012). An event log is composed of a list of events, where all data extracted from systems is converted to this log. Each event should have a minimal set of attributes: a case id (a unique number to represent the case), an activity name to indicate the performed action, and the date and time when the action was executed (Rodrigues et al., 2017).

We have tested our approach using the event log of BPI Challenge 2017, a real-life log taken from a financial institution. The BPI Challenge provided an event log that contains all applications filed in 2016, and at the beginning of 2017. In total, there are 31,509 loan applications, *i.e.* cases. Our goal with the application is to find patterns and correlations between different cases based on the similarity among attributes that define a process, because this is an important task in process discovery.

With this event log, for all applications, the available data (attributes) are the following:

- Requested load amount (in Euro),
- The application type,
- The reason for the loan request (Loan Goal), and
- An application ID.

For all offers, the following data are available:

- An offer ID
- The offered amount,
- The initial withdrawal amount,
- The number of payback terms agreed to,
- The monthly costs,
- The customer's credit score,
- The employee who created the offer,
- Whether the offer was selected, and
- Whether the customer accepted the offer.

For each uniquely identifiable event, the employee who triggered the event is recorded, as well as time stamp and life-cycle information. In this dataset, there are more than 1.2 million events, and each event corresponds to one of the 26 possible activities of the process.

Each application is a single case in this dataset and, for each case, a number of offers can be sent to a client. A case may have one of three possible endings in the event log: Approved (*A_Pending*), Denied (*A_Denied*), or Cancelled (*A_Cancelled*). In the event log, 100 cases were undefined, meaning that none of the possible endings had been reached. Because of this, they were discarded in our experiments. In our preliminary experiments, we performed tests with the entire data set, *i.e.*, 31,409 cases.

With this data, we aim to assess our approach usefulness in answering questions of common problems in the domain, by clustering data and analyzing patterns in each of the attributes. This can be considered an initial step for process discovery, and a meticulous analysis of the filtered data is needed afterwards.

We transform the event log into a dataset, where the rows represent the cases and the columns characterize each case, based on the following features: *Credit Score*, *Requested Amount*, *Number of Offers*, and *Loan Goal*. We selected these features to find similarities between cases. Also, we added the pairwise Jaccard index and Levenshtein distance as additional features.

We use MDS to explore the data. As shown in Figure 5, we experimented with different projections, trying to identify visual patterns and relations between the cases. We experimented with different weights for the dissimilarity metric, in order to evaluate the

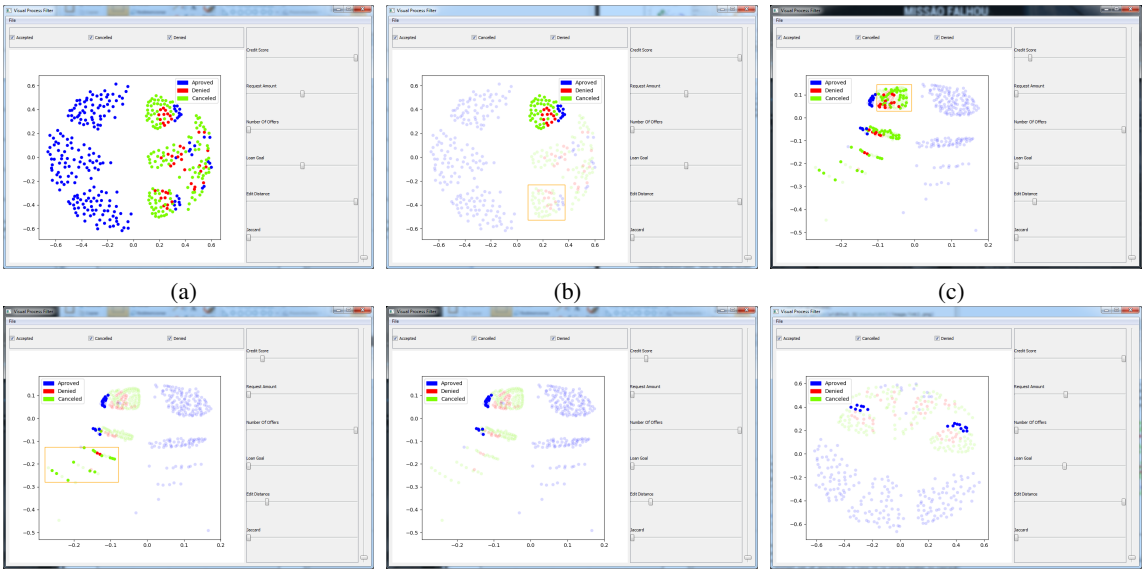

Figure 5: Exploring the data and selecting cases using MDS dimensionality reduction. We can select and deselect cases changing the visualization. For each choice of weights for each feature, we maintain the selection of the cases. In the Figure (a)(b), we start selecting two groups of points. With a different set of weights, as in Figure (c), we can explore different visualizations maintaining the same selected points. In the Figures (d)(e), we deselect some other points and then, in Figure (f), we adjust the weights to visualize the similar projection of (a), but now with a smaller set of selected points.

data and find which attributes had a grouping factor in the dataset.

Using our prototype, it is possible to manually select a subset of cases using click-and-drag interaction and export the selection to a CSV file to load it into a Process Mining software, such as Disco or ProM. Figure 6 shows the process flow using Disco with all the 31,409 valid cases and with a sublog obtained with our filtering tool.

Unfortunately, MDS is not efficient when dealing with a large number of cases, both in terms of computational time and memory used. In our study, we projected 31,409 cases, with considerable time spent for each projection, in average 2 hours for each experiment and 60 GB of memory used to store all data structures used in this technique. We perform our test in a computer with an Intel core i7-5820K CPU@3.30GHz, 64GB of memory, 1TB of hard disc and a graphics card Nvidia Titan Xp DDR5 with 12 GB of memory. However, for smaller dataset, the MDS does not have such problem. Table 1 shows the computational time for the same dataset with less cases.

As a quality measure, we considered the stress of the projection. This measure depends on the weights chosen by the user in the dissimilarity equation but, in the best case, considering only the features of Levenshtein distance and loan goal, the stress is 0.15.

Table 2 shows the weights assigned to each attribute of the dataset when calculating the pairwise dissimilarity between the cases. Using these weights, we projected the full set of cases. The resulting projection is shown in Figure 7. We then selected 6 clusters using our prototype tool, also shown in Figure 7.

Table 1: Run time for each test.

| | Number of cases | time (min) |
|---|---|---|
| 1 | 1000 | 0.366 |
| 2 | 2000 | 0.576 |
| 3 | 5000 | 2.010 |
| 4 | 10000 | 6.880 |
| 5 | 20000 | 31.400 |
| 6 | 31409 | 130.02 |

Table 2: Parameters defined to filter the 31409 cases.

| | Attribute | Value |
|---|---|---|
| 1 | Loan Goal | 1.00 |
| 2 | Credit Score | 0.50 |
| 3 | Number of Offers | 0.00 |
| 4 | Requested Amount | 0.50 |
| 5 | Levenshtein Distance | 0.00 |
| 6 | Jaccard Index | 1.00 |

In order to validate our approach, we used a clustering algorithm on the complete event log to automatically find 6 clusters. We used a version of K-Medoids (Kaufman and Rousseeuw, 2009) named

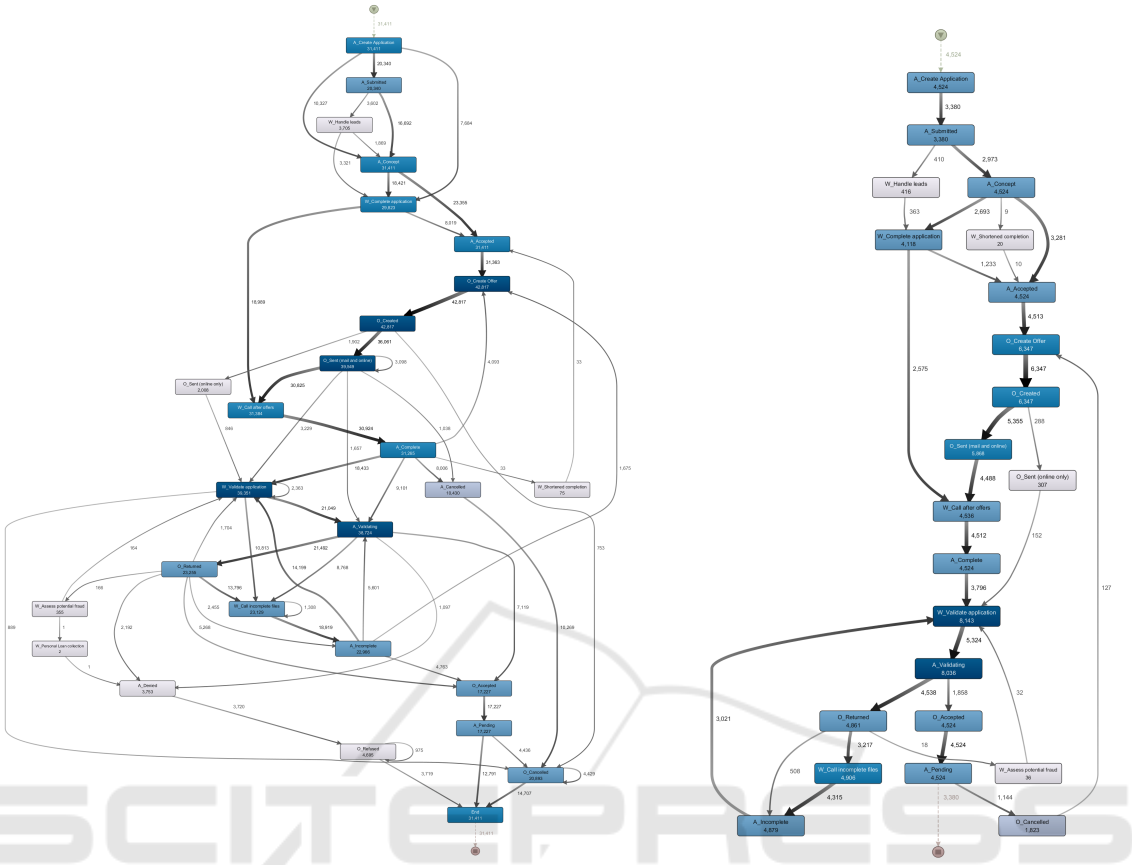

(a) (b)

Figure 6: Difference between the process map using all 31,409 cases (a) and the filtered sublog(b).

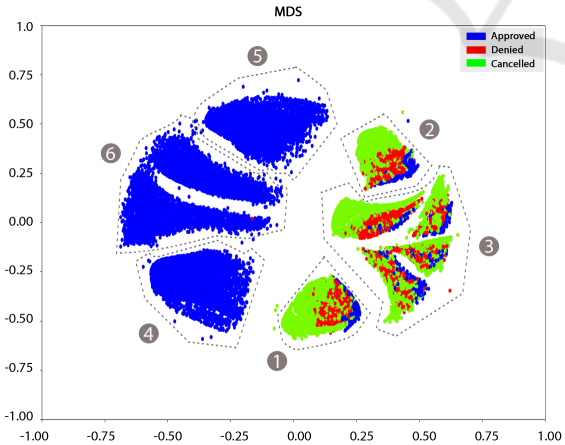


Figure 7: Filtered image with 6 clusters selection using the parameters specified in Table 2 with MDS.

Partitioning Around Medoids (PAM). The algorithm searches for $k$ *representative objects* i.e. *medoids* of the clusters, which minimize the sum of pairwise dissimilarities between each object (case) and the closest medoid. The $k$ clusters are constructed by assigning each object of the dataset to the nearest representative object.

To evaluate how cohesive the clusters are, we calculated their entropy. Shannon's entropy (Shannon and Weaver, 1963) quantifies this cohesiveness, *i.e.* the uncertainty associated with a discrete random variable $X$ with $N$ possible outcomes (Lopes and Barbosa, 2015). Equation 4 describe this measure.

$$H^{(S)}[P] = -\sum_{j=1}^{N} p_j ln(p_j) \tag{4}$$

Where $p_j$ is the probability of the outcome $j$ appearing in the variable. Since our dissimilarity measure is normalized, we decided to use the normalized version of the Shannon entropy, as shown in Equation 5.

$$H^{(S)}[P] = \frac{H^{(S)}[P]}{H^{(S)}[P_e]} = -\sum_{j=1}^{N} \frac{p_j ln(p_j)}{ln(n)} \tag{5}$$

Where $H^{(S)}[P] \in [0,1]$. When the entropy is close to 0, the cluster is homogeneous. Conversely, when it is closer to 1, the cluster is heterogeneous.

Using K-Medoids with $k = 6$ and $31,397$, which is the number of clusters and data points, respectively, obtained using our filtering tool, we calculated the entropy of each cluster with respect to the variables. Figure 10 shows this result.

Similarly, we calculated the entropy for each of the visually selected clusters. Figure 11 shows this result. It is important to note that we use a gradient color scale to identify the entropy. Lower entropies (the most interesting ones for this study) appear in shades of blue, where the darker blue is entropy close to 0. The higher (less interesting) entropies appear in shades of red, where the darker red is entropy near 1.

In general, the separation of data points through the filtering tool resulted in clusters with low uncertainty value for the Goal and similar to Credit Score variables, when compared to K-Medoids.

To assist in the descriptive analysis of clusters, we calculated the frequency of the values in each of the variables of the MDS approach. The result can be seen in Figure 12, where each row represents a cluster. Histogram colors match entropy colors.

From this moment it is possible to describe the clusters defined by MDS method (see Figures 7, 11 and 12).

Cluster 1 is characterized by a higher percentage of cases that were Cancelled (10.817%, row 1 in Table 3) at the end of the process. Regarding Goal and Credit Score, the entropy is 0, meaning there is no uncertainty (Figure 11). In this cluster, all cases have *Goal* = Car and Credit Score in the range $[0,500)$ (row 1 in Figure 12). Entropy increases for the Number of Offers (0.42), where most cases received 1 offer, and also to the Requested Amount (0.77), where the amounts requested are heavily distributed between cases.

Cluster 2 has similar characteristics to Cluster 1 in terms of Cancelled cases (7.383%, row 2 in Table 3) and entropy of the same variables (Figure 11). However, the purpose of the loan for this cluster is Home Improvement (row 2 in Figure 12). This is evident when we look at the clusters of Figure 7: they are visually alike but distant.

Cluster 3 also has mostly Cancelled cases (15.009%, row 3 in Table 3). The entropy is high for the variables considered, except for Credit Score, which is 0 (Figure 11). In this cluster all cases have Credit Score in the range $[0,500)$ (row 3 in Figure 12).

Cluster 6, in spite of having practically all Approved cases (20.350%, row 6 in Table 3), has high entropy in all considered variables (Figure 11). Only one case was not approved, getting a Denied endpoint. This behavior caught our attention and, for this reason, we analyze this particular case. We detected that the values of the variables are within the limits of each of these clusters (red dots in Figure 12 represents this particular case), but it presented a path between the events totally different from the rest of the cluster. This, in fact, proves that the MDS can group cases according to the similarity of the variables, regardless of the defined paths.

Clusters 4 and 5, again, have similar characteristics. Both have high entropies, very close to each other (Figure 11). The types and frequency of values for the Credit Score, Number of Offers, and Requested Amount variables are very similar too (rows 4 and 5, respectively in Figure 12). However, Cluster 4 has *Goal* = Car and Cluster 5, *Goal* = Home improvement. Again we can compare this behavior with the visual clusters. These clusters are distant but similarly shaped (Figure 7). As we can see in Figure 6, the sublog represents the process obtained with the filtered log representing cluster 4.

In general, we can verify that the Credit Score separates the clusters in two groups by the diagonal, where the high entropy are on the left-hand side and the low entropy are on the right-hand side in Figure 7.

In order to visualize the results of the K-Medoids clustering, we plotted the projections of $31,397$ cases selected using our visual approach and colored the points by their assigned K-Medoids cluster label. Figure 8 shows this result.

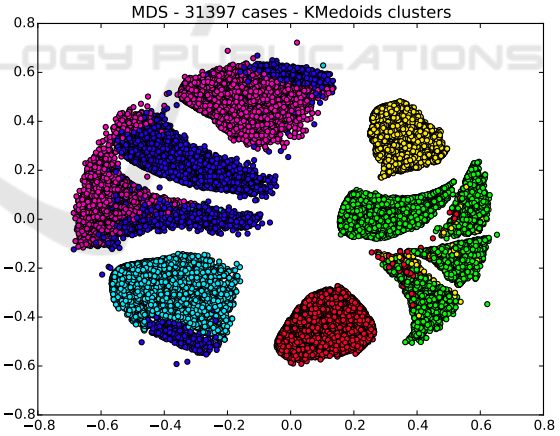


Figure 8: MDS projection of the $31,397$ cases colored by their K-Medoids assigned cluster.

K-Medoids obtains clusters with silhouette measure (Rousseeuw, 1987) equivalent to our approach, as seen in tables 4 and 5, but it visually scrambles some of the cases (Figure 8). Using the same colors of the K-Medoids clusters, we painted the concordance matrix in Figure 9, showing how the data points are distributed among clusters of each approach. We also quantified the amount of information shared between K-Medoids clustering results and the visual clusters

Table 3: Cluster characterization of MDS approach in terms of process (* %with respect to all 31,397 cases).

| Cluster | #Cases | #Variants | Approved | %Approved* | Denied | %Denied | Canceled | %Canceled |
|---|---|---|---|---|---|---|---|---|
| 1 | 5075 | 656 | 556 | 1.771 | 1123 | 3.577 | 3396 | 10.817 |
| 2 | 3724 | 570 | 569 | 1.812 | 837 | 2.666 | 2318 | 7.383 |
| 3 | 7349 | 949 | 846 | 2.695 | 1791 | 5.705 | 4712 | 15.009 |
| 4 | 4524 | 851 | 4524 | 14.410 | 0 | 0.000 | 0 | 0.000 |
| 5 | 4335 | 850 | 4335 | 13.808 | 0 | 0.000 | 0 | 0.000 |
| 6 | 6390 | 1482 | 6389 | 20.350 | 1 | 0.003 | 0 | 0.000 |

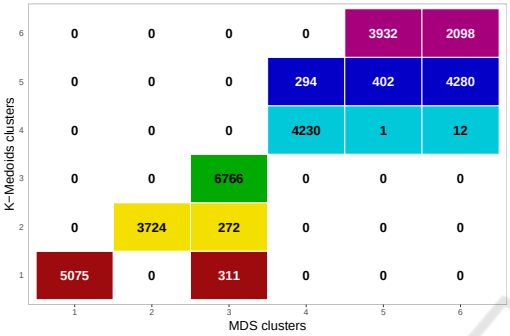


Figure 9: Frequency of datapoints in each cluster. Colors represent the relation between clusters in K-Medoids and MDS.

Table 4: K-Medoids silhouette.

| Method | Cl | Mean(sd) | Minvalue | Maxvalue |
|---|---|---|---|---|
| KMed. | 1 | 0.270 (0.090) | -0.105 | 0.550 |
| | 2 | 0.271 (0.093) | -0.109 | 0.543 |
| | 3 | 0.060 (0.049) | -0.019 | 0.241 |
| | 4 | 0.258 (0.049) | -0.083 | 0.477 |
| | 5 | 0.115 (0.077) | -0.011 | 0.342 |
| | 6 | 0.118 (0.085) | -0.021 | 0.352 |

obtained with our prototype. To do this, we calculated the Normalized Mutual Information Index (NMII) (Strehl and Ghosh, 2002). We obtained a NMII value of 0.84, meaning that 84% of the cases fall into the same groups in the two approaches. Also, as we can see in Table 6, there is high variability for some attributes, especially the Requested Amount. This may explain the high entropy values for this attribute.

The Loan Goal attribute was not included in Table 6 because it is a categorical variable with 14 different classes.

Table 5: MDS silhouette.

| Method | Cl | Mean(sd) | Minvalue | Maxvalue |
|---|---|---|---|---|
| MDS | 1 | 0.306 (0.049) | 0.236 | 0.583 |
| | 2 | 0.311 (0.044) | 0.251 | 0.582 |
| | 3 | 0.068 (0.040) | -0.006 | 0.219 |
| | 4 | 0.220 (0.083) | -0.137 | 0.456 |
| | 5 | 0.215 (0.093) | -0.150 | 0.472 |
| | 6 | 0.086 (0.054) | -0.008 | 0.243 |

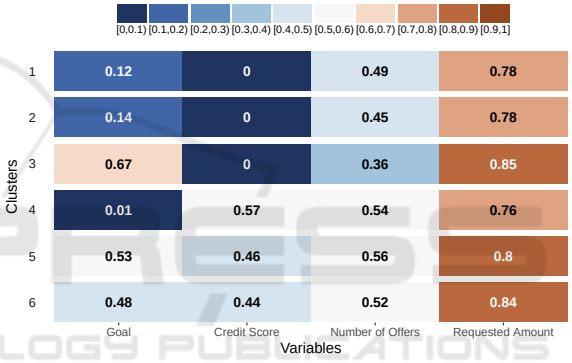


Figure 10: Entropy value of each cluster by variable in K-Medoids approach.

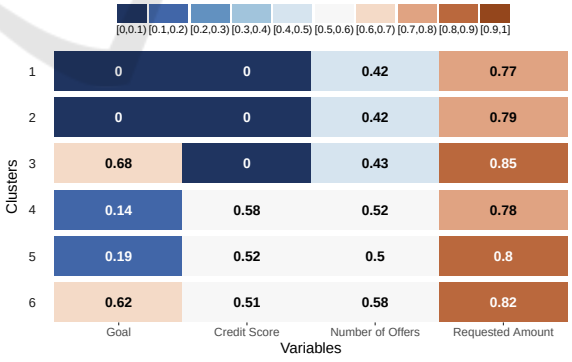


Figure 11: Entropy value of each cluster by variable in MDS projection chart.

## 6 CONCLUSION

In this paper, we proposed a novel approach for understanding and filtering cases of general event logs. Our approach is based on evaluating the similarity between pairs of cases and using multidimensional projection techniques to plot those cases into a 2D chart. Using the BPI Challenge 2017 data, our approach shows that we can not only select some cases, but also see some correlation of the data, projected into our reduced space. Also, this filtering approach allows us to decompose a large event log into small pieces and analyze them separately, a useful approach


Figure 12: Characteristics of each cluster, by variable. Histogram colors match entropy colors. For the Loan Goal variable, which is a categorical variable, the values are abbreviated as follows: UN = Unknown, TP = Tax payments, RD = Remaining debt home, OT = Other, see explanation, NA = Not specified, MO = Motorcycle, HI = Home improvement, EP = Extras pending limit, EL = Existing loan take over, DR = Debt restructuring, CC = Caravan/Camper, CA = Car, BO = Boat and BG = Business goal.

Table 6: Summary results for the numeric attributes of the BPI 2017 dataset.

| Statistics | Credit Score | Nb. Offer | R. Amount |
|---|---|---|---|
| Min. | 0.000 | 1.000 | 0.00 |
| 1st Qu. | 0.000 | 1.000 | 6000.00 |
| Median | 0.000 | 1.000 | 12500.00 |
| Mean | 436.100 | 1.363 | 16210.00 |
| 3rd Qu. | 901.000 | 2.000 | 21000.00 |
| Max. | 1145.000 | 10.000 | 450000.00 |

in the process discovery field (Verbeek et al., 2017).

We are still making improvements to our prototype based on interesting demands that should help to understand the process and to filter cases. As future work, we want to incorporate our tool as a ProM plug-in. We also intend to include Local Affine Multidimensional Projection (LAMP) (Joia et al., 2011; Pagliosa et al., 2015) in our prototype, which will enable us to set a group of control points and dynamically project new instances. Another interesting idea is to incorporate attribute-level linkage, similar to the analysis we performed in Section 5, to the prototype itself. This way, an analyst may quickly discover which attributes contribute to the dataset variability and, thus, fine-tune the attribute weights for the dissimilarity metric.

## ACKNOWLEDGEMENTS

We thank Conselho Nacional de Desenvolvimento Científico e Tecnológico (CNPq) and Coordenação de Aperfeiçoamento de Pessoal de Nível Superior (CAPES) for partially financing this research.

## REFERENCES

De Koninck, P. and De Weerdt, J. (2016). Multi-objective trace clustering: finding more balanced solutions. In *International Conference on Business Process Management*, pages 49–60. Springer.

Hunter, J. D. (2007). Matplotlib: A 2d graphics environment. *Computing In Science & Engineering*, 9(3):90–95.

Jaccard, P. (1901). Étude comparative de la distribution florale dans une portion des alpes et des jura. *Bull Soc Vaudoise Sci Nat*, 37:547–579.

Joia, P., Coimbra, D., Cuminato, J. A., Paulovich, F. V., and Nonato, L. G. (2011). Local affine multidimensional projection. *IEEE Transactions on Visualization and Computer Graphics*, 17(12):2563–2571.

Kaufman, L. and Rousseeuw, P. J. (2009). *Finding groups in data: an introduction to cluster analysis*, volume 344. John Wiley & Sons.

Kruskal, J. B. and Wish, M. (1978). *Multidimensional Scaling*, volume 31.

Levenshtein, V. I. (1966). Binary codes capable of correcting deletions, insertions, and reversals. In *Soviet physics doklady*, volume 10, pages 707–710.

Lopes, H. and Barbosa, S. (2015). *Learning and Inferring: Festschrift for Alejandro Frery*, chapter Uncertainty Measures and the concentration of probability density functions. College Publications.

Low, W. Z., Van der Aalst, W. M., ter Hofstede, A. H., Wynn, M. T., and De Weerdt, J. (2017). Change visualisation: Analysing the resource and timing differences between two event logs. *Information Systems*, 65:106–123.

Maaten, L. v. d. and Hinton, G. (2008). Visualizing data using t-sne. *Journal of Machine Learning Research*, 9(Nov):2579–2605.

Mendling, J., Baesens, B., Bernstein, A., and Fellmann, M. (2017). Challenges of smart business process management: An introduction to the special issue.

Mining, P. (2014). Automated process discovery software for professionals-fluxicon disco. *Adres: http://fluxicon. com/disco/Erişim Tarihi*, 11.

Mises, R. and Pollaczek-Geiringer, H. (1929). Praktische verfahren der gleichungsauflösung. *ZAMM-Journal of Applied Mathematics and Mechanics/Zeitschrift für Angewandte Mathematik und Mechanik*, 9(1):58–77.

Pagliosa, P., Paulovich, F. V., Minghim, R., Levkowitz, H., and Nonato, L. G. (2015). Projection inspector: Assessment and synthesis of multidimensional projections. *Neurocomputing*, 150:599–610.

Pedregosa, F., Varoquaux, G., Gramfort, A., Michel, V., Thirion, B., Grisel, O., Blondel, M., Prettenhofer, P., Weiss, R., Dubourg, V., et al. (2011). Scikit-learn: Machine learning in python. *Journal of Machine Learning Research*, 12(Oct):2825–2830.

Rodrigues, A. M. B., Almeida, C. F. P., Saraiva, D. D. G., Moreira, F. B., Spyrides, G. M., Varela, G., Krieger, G. M., Peres, I. T., Dantas, L. F., Lana, M., Alves, O. E., Franca, R., Neira, R. A. Q., Gonzalez, S. F., Fernandes, W. P. D., Barbosa, S. D. J., Poggi, M., and Lopes, H. (2017). Stairway to value: mining a loan application process. Technical report, Pontifícia Universidade Católica do Rio de Janeiro.

Rousseeuw, P. J. (1987). Silhouettes: a graphical aid to the interpretation and validation of cluster analysis. *Journal of computational and applied mathematics*, 20:53–65.

Shannon, C. E. and Weaver, W. (1963). *A Mathematical Theory of Communication*. University of Illinois Press, Champaign, IL, USA.

Strehl, A. and Ghosh, J. (2002). Cluster ensembles—a knowledge reuse framework for combining multiple partitions. *Journal of machine learning research*, 3(Dec):583–617.

Tiwari, A., Turner, C. J., and Majeed, B. (2008). A review of business process mining: state-of-the-art and future trends. *Business Process Management Journal*, 14(1):5–22.

Van Der Aalst, W. (2012). Process mining. *Communications of the ACM*, 55(8):76–83.

Van der Aalst, W., Weijters, T., and Maruster, L. (2004). Workflow mining: Discovering process models from event logs. *IEEE Transactions on Knowledge and Data Engineering*, 16(9):1128–1142.

Van der Aalst, W. M. (2016). *Process mining: data science in action*. Springer.

Van der Aalst, W. M. and Weijters, A. (2004). Process mining: a research agenda. *Computers in industry*, 53(3):231–244.

Verbeek, H., Buijs, J., Van Dongen, B., and van der Aalst, W. M. (2010). Prom 6: The process mining toolkit. *Proc. of BPM Demonstration Track*, 615:34–39.

Verbeek, H., Van der Aalst, W., and Munoz-Gama, J. (2017). Divide and conquer: A tool framework for supporting decomposed discovery in process mining. *The Computer Journal*, pages 1–26.

Wattenberg, M., Vigas, F., and Johnson, I. (2016). How to use t-sne effectively. *Distill*.